



EXPERIMENTAL RESULTS AND DISCUSSIONS

5.1 Introduction.

The experiments to measure thermal fields can be classified into two categories:

1. Tests to find the effects of the size of nozzle on the temperature distribution.
2. Tests to determine how longshore currents influence the mixing process.

Table 5.1 depicts the fifteen experimental conditions investigated. For each experimental run, surface isotherms in the vicinity of discharge point are plotted and the results are expressed in terms of the areas encircled by the isothermal lines of temperatures 0.5, 1.0, 1.5. and 2.0°C greater than the ambient. Figures 5.1 - 5.15 show the isothermal lines obtained from each run of the experiments. Figures 5.16 - 5.20 display the vertical variations in temperature at the point 30 m.* downstream from the point of discharge. The relation between the area encircled by the isothermal line and the current speed for the given size of nozzle is illustrated in figures 5.21 - 5.23 . A summary of the experimental results is tabulated in Table 5.2 .

* The distance referred to in this chapter is the distance in prototype not in model.

TABLE 5.1

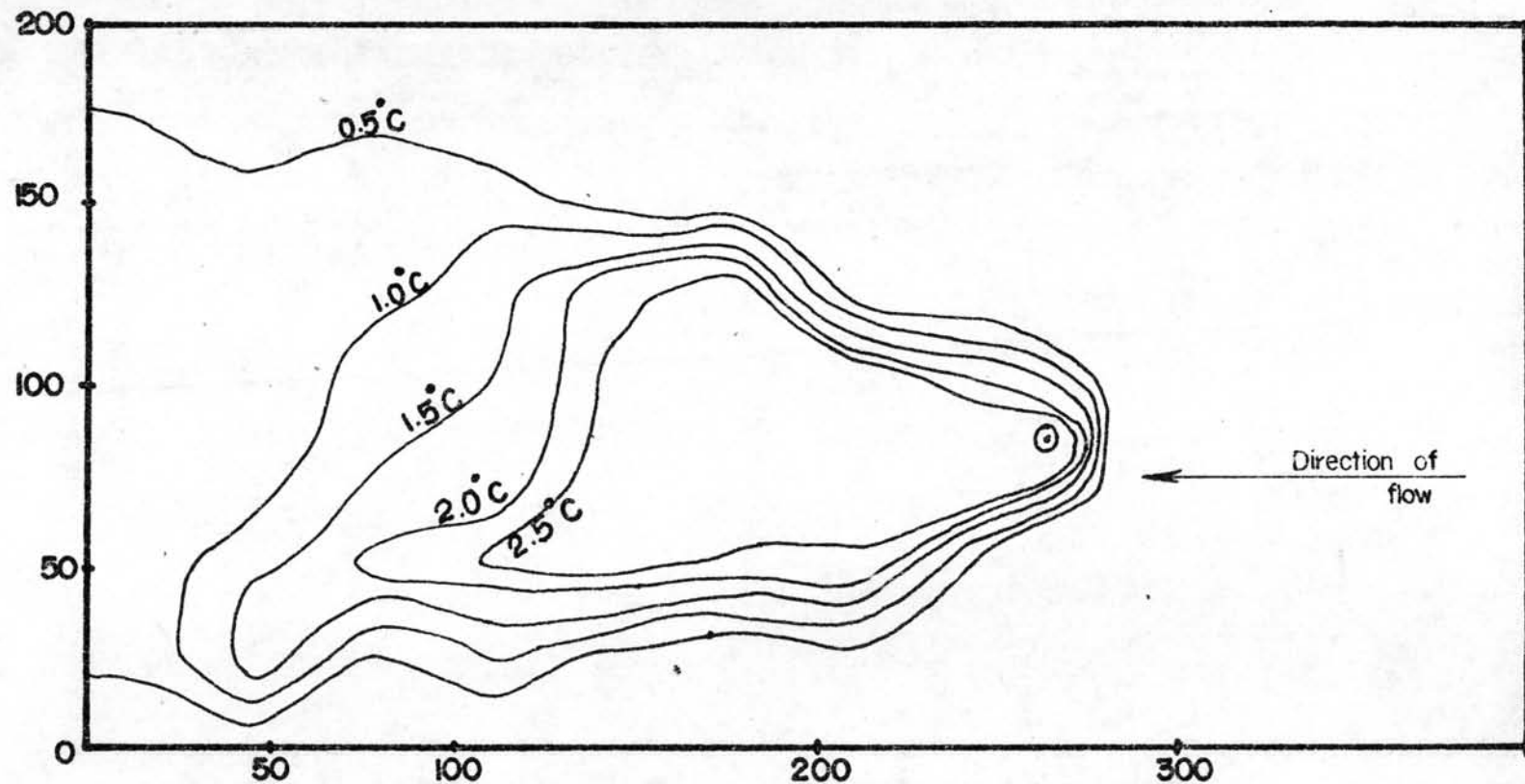
THE EXPERIMENTAL CONDITIONS INVESTIGATED

Run No	Nozzle Diameter (m)	Current (m/sec)	Condenser Discharge (m ³ /sec)
1	3	0.6	34.9
2	4	0.6	34.9
3	5	0.6	34.9
4	3	0.8	34.9
5	4	0.8	34.9
6	5	0.8	34.9
7	3	0.9	34.9
8	4	0.9	34.9
9	5	0.9	34.9
10	3	1.0	34.9
11	4	1.0	34.9
12	5	1.0	34.9
13	3	1.2	34.9
14	4	1.2	34.9
15	5	1.2	34.9

TABLE 5.2

THE EXPERIMENTAL RESULTS

Run No.	Ambient Current (m/sec)	Nozzle Diameter (m)	Jet Velocity (m/sec)	Area within			
				0.5 °C isotherm (m ²)	1.0 °C isotherm (m ²)	1.5 °C isotherm (m ²)	2.0 °C isotherm (m ²)
1	0.6	3	4.93	-	20,520	14,400	8,120
2	0.6	4	2.78	-	12,720	4,800	1,200
3	0.6	5	1.78	31,600	17,200	6,120	1,800
4	0.8	3	4.93	24,800	15,600	10,520	6,200
5	0.8	4	2.78	25,800	11,960	2,400	520
6	0.8	5	1.78	25,640	12,800	5,400	680
7	0.9	3	4.93	22,080	15,000	7,600	1,880
8	0.9	4	2.78	20,000	6,000	1,400	800
9	0.9	5	1.78	23,600	8,880	4,720	2,200
10	1.0	3	4.93	18,840	11,840	7,560	3,000
11	1.0	4	2.78	25,200	13,000	6,040	2,800
12	1.0	5	1.78	22,120	7,280	2,560	960
13	1.2	3	4.93	14,800	7,360	4,600	3,240
14	1.2	4	2.78	12,320	10,840	4,240	1,240
15	1.2	5	1.78	13,760	6,840	3,320	320



Nozzle Diameter 3 metre

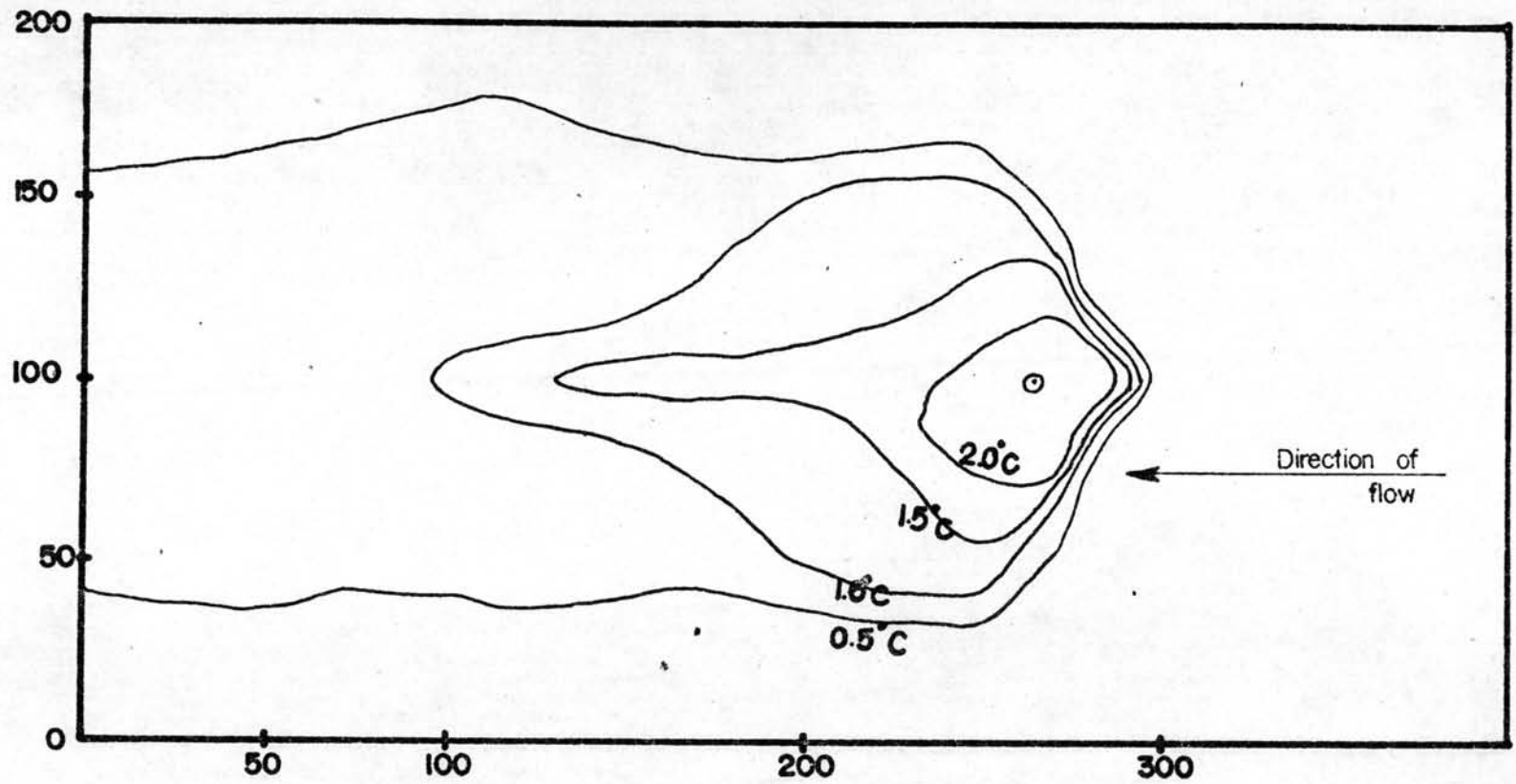
Current Speed 0.6 m/sec.

Discharge Temperature above Ambient Temperature 10°C

⊙ - Point of Discharge

SCALE
in metre 0 50 100

FIG. 5.1 SURFACE TEMPERATURE RISE CONTOURS IN THE VICINITY OF THE DISCHARGE FOR RUN NO. I



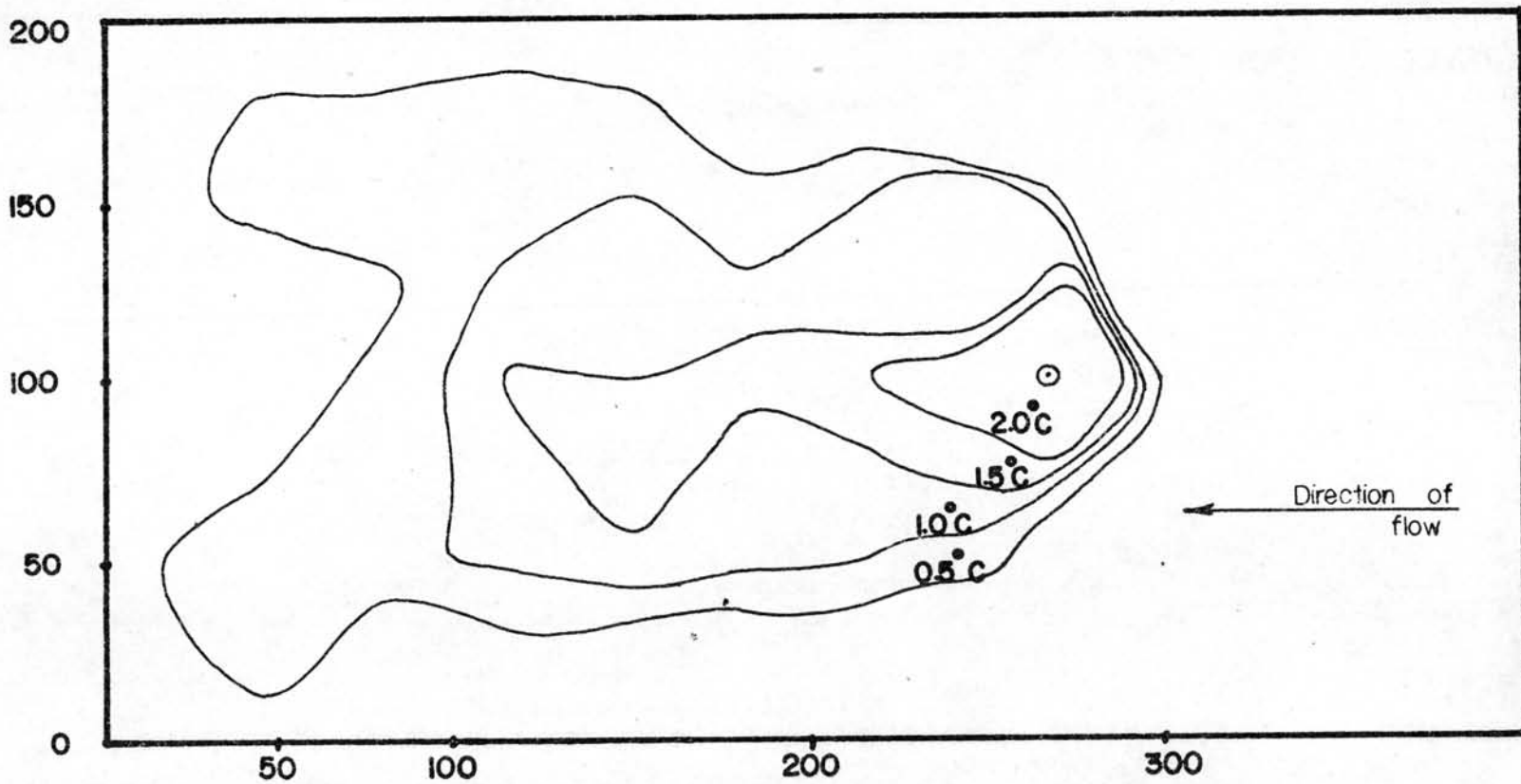
Nozzle Diameter 4 metre
 Current Speed 0.6 m/sec
 Discharge Temperature above Ambient Temperature 10 °C
 ⊙ - Point of Discharge



FIG. 5.2 SURFACE TEMPERATURE RISE CONTOURS IN THE VICINITY OF THE DISCHARGE FOR RUN NO.2

41

42

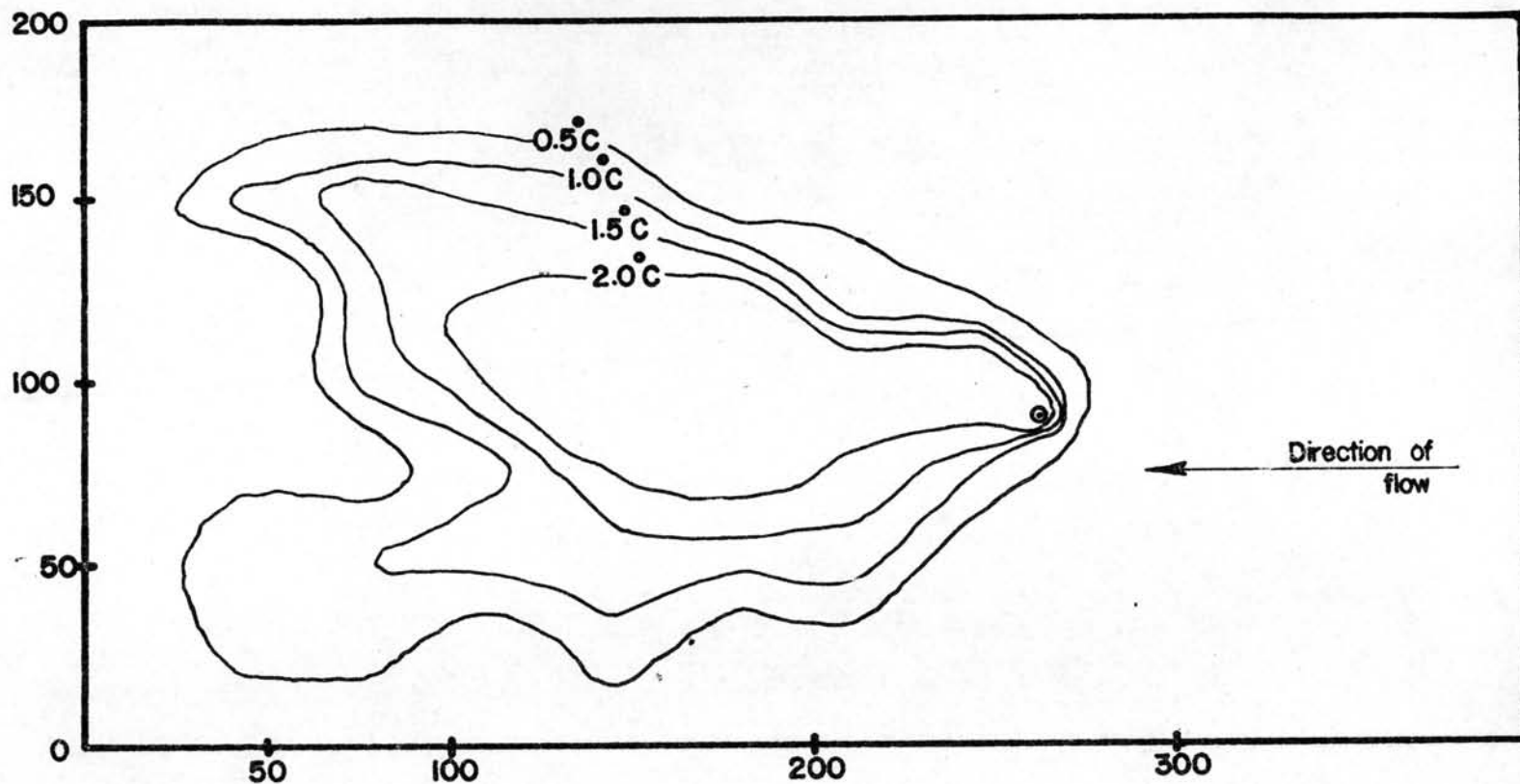


Nozzle Diameter 5 metre
Current Speed 0.6 m/sec.
Discharge Temperature above Ambient Temperature 10°C
⊙ - Point of Discharge

SCALE
in metre :



Fig. 5.3 SURFACE TEMPERATURE RISE CONTOURS IN THE VICINITY OF THE DISCHARGE FOR RUN NO. 3



Nozzle Diameter 3 metre

Current Speed 0.8 m/sec.

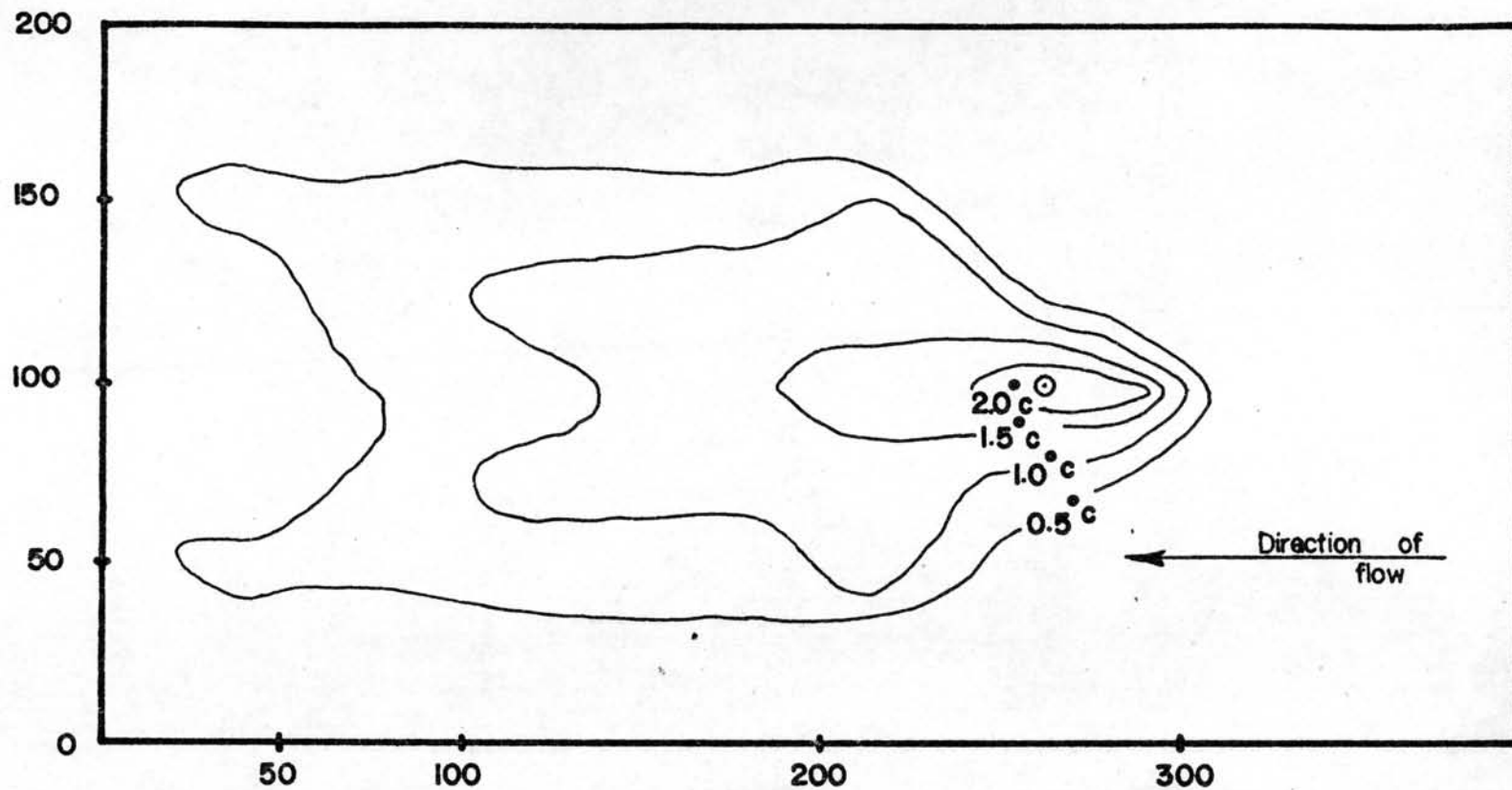
Discharge Temperature above Ambient Temperature 10°C

⊙ - Point of Discharge

SCALE
in metre



FIG. 5.4 SURFACE TEMPERATURE RISE CONTOURS IN THE VICINITY OF THE DISCHARGE FOR RUN NO. 4



Nozzle Diameter 4 meter
Current Speed 0.8 m/sec
Discharge Temperature above Ambient Temperature 10° c
⊙ - Point of Discharge

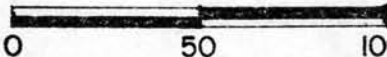
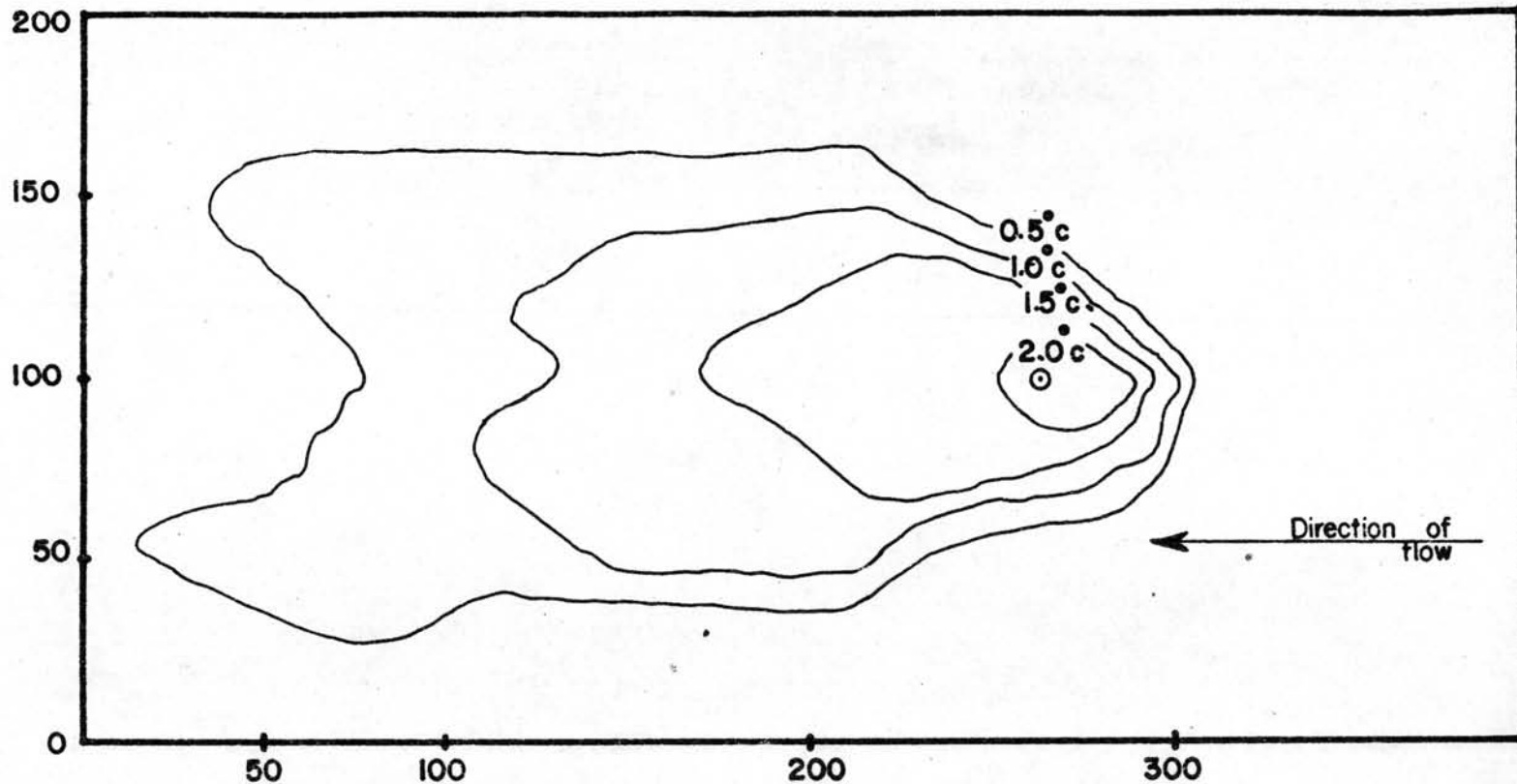
SCALE
in metre : 

FIG. 5.5 SURFACE TEMPERATURE RISE CONTOURS IN THE VICINITY OF THE DISCHARGE FOR RUN NO. 5

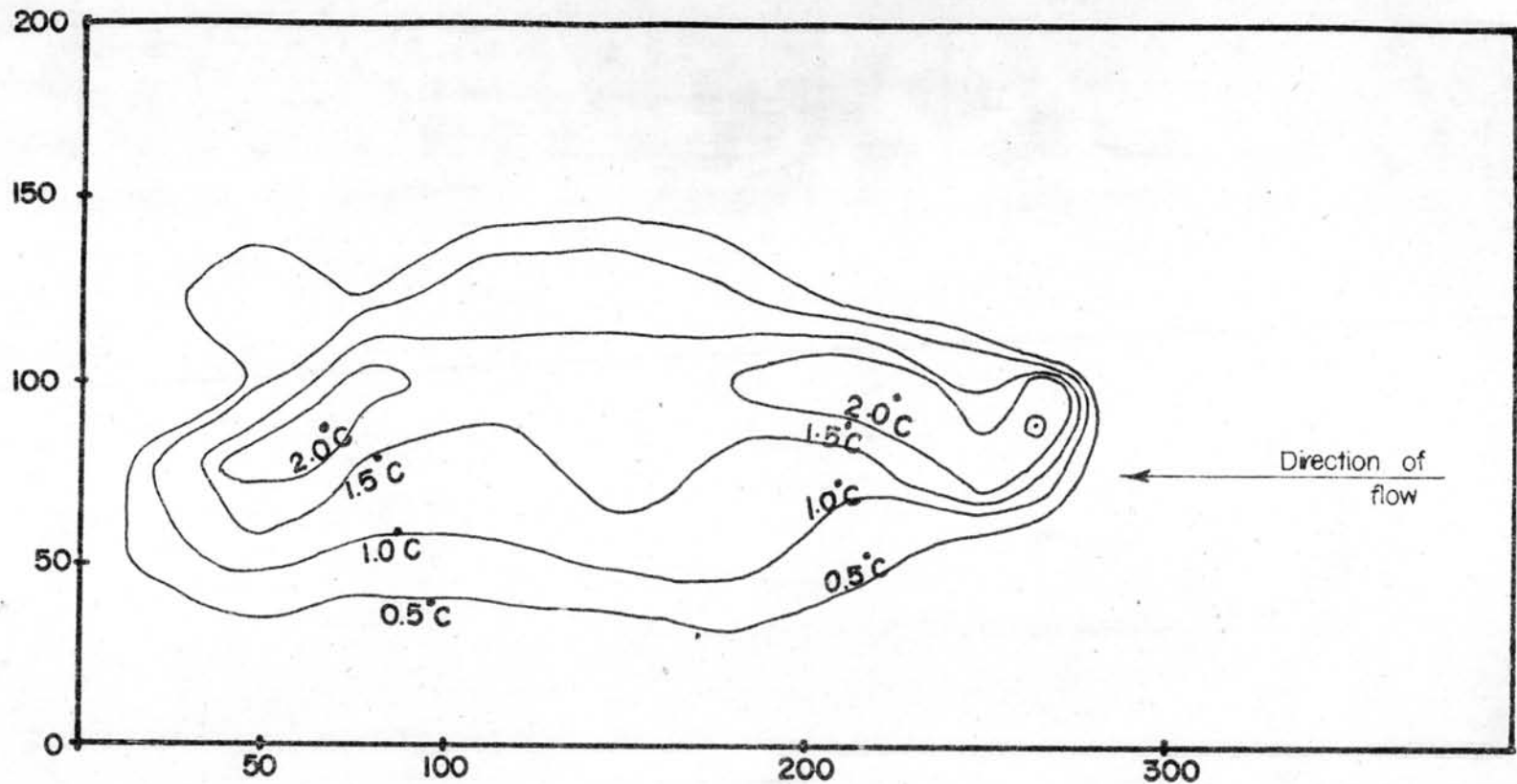


Nozzle Diameter 5 metre
 Current Speed 0.8 m/sec
 Discharge Temperature above Ambient Temperature 10°C
 ⊙ - Point of Discharge



FIG. 5.6 SURFACE TEMPERATURE RISE CONTOURS IN THE VICINITY
 OF THE DISCHARGE FOR RUN NO. 6

-45-



Nozzle Diameter 3 metre

Current Speed 0.9 m/sec

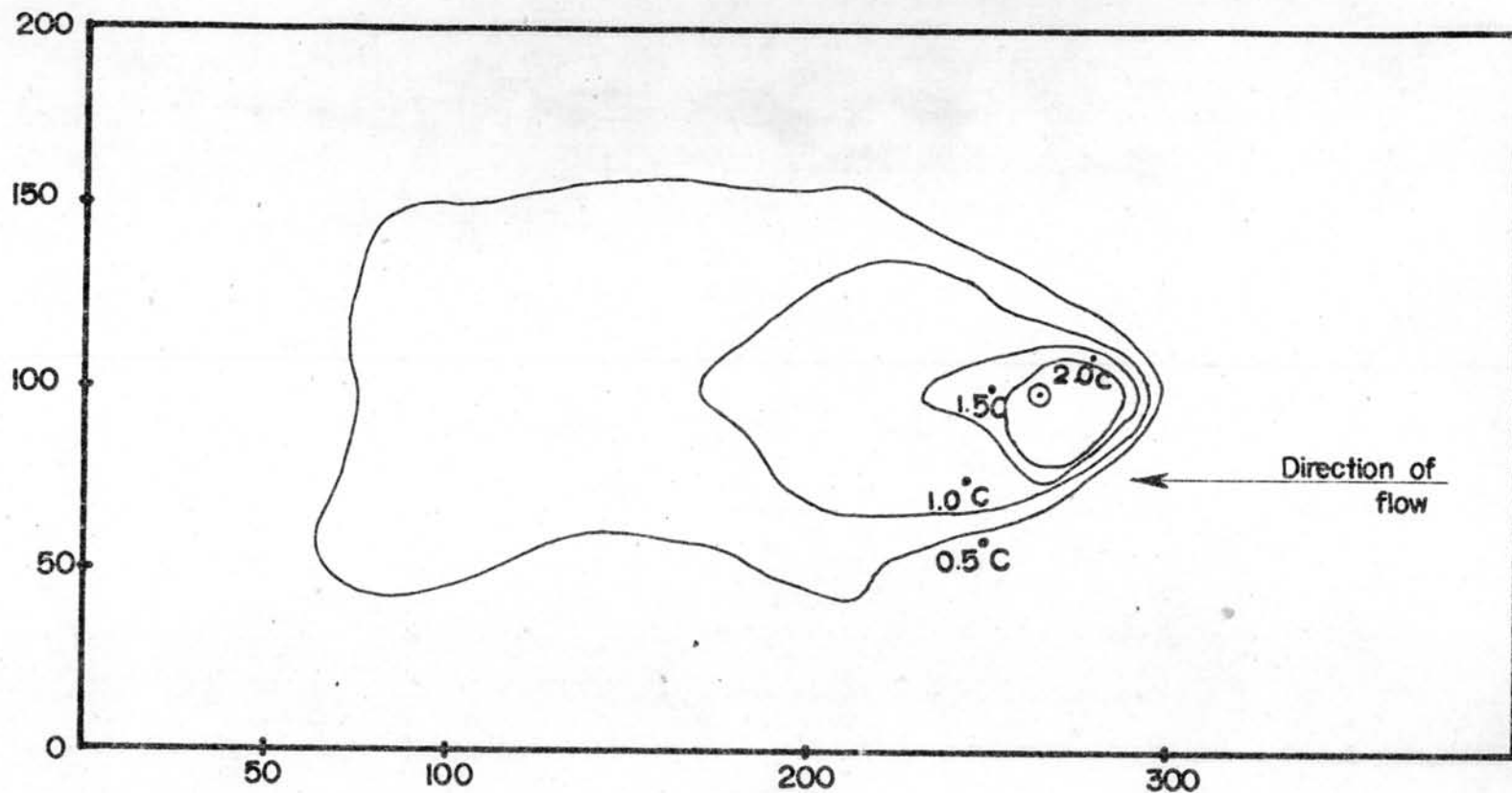
Discharge Temperature above Ambient Temperature 10°C

⊙ - Point of Discharge

SCALE
in metre :



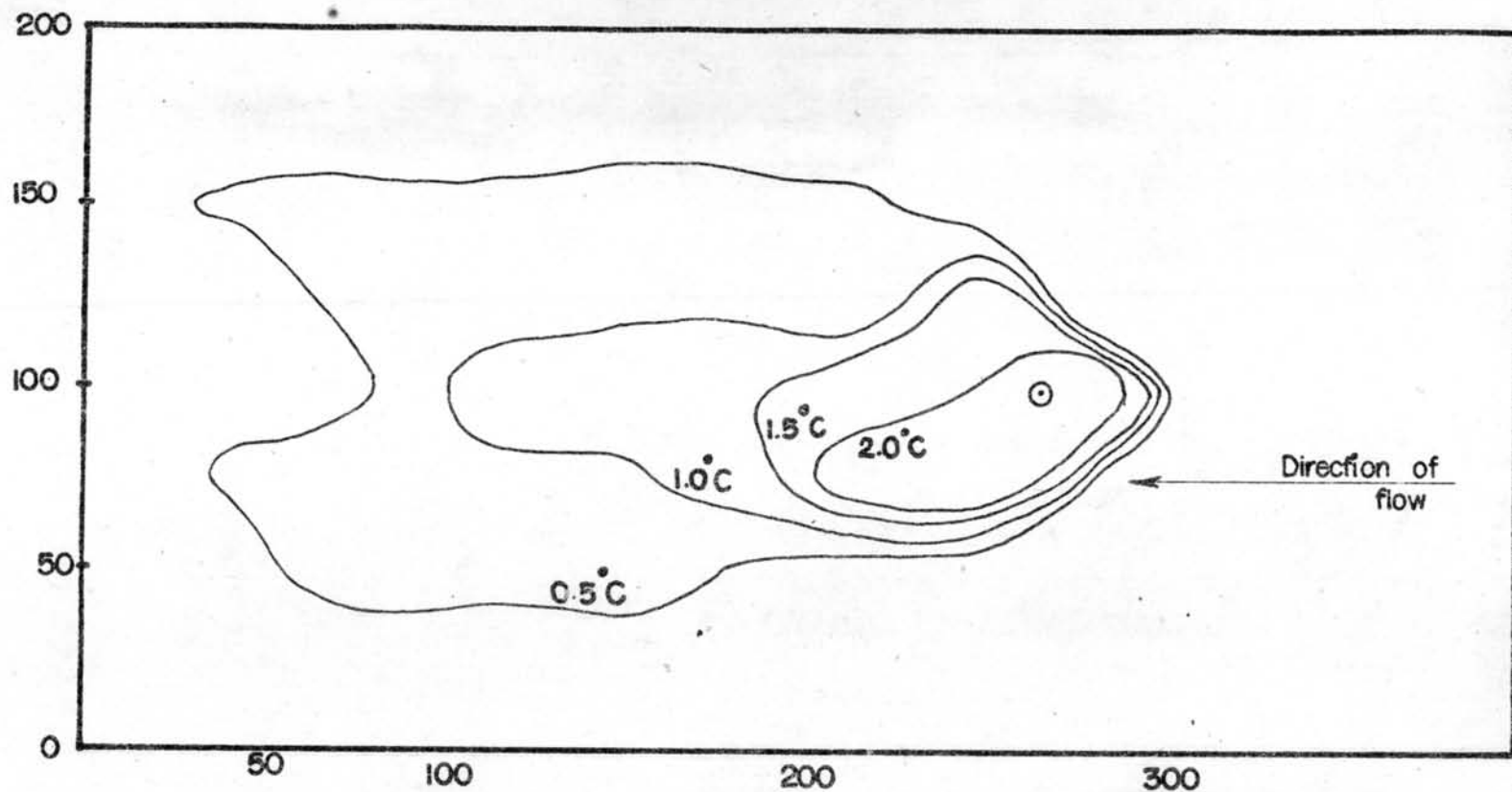
FIG. 5.7 SURFACE TEMPERATURE RISE CONTOURS IN THE VICINITY OF THE DISCHARGE FOR RUN NO. 7



Nozzle Diameter 4 metre
 Current Speed 0.9 m/sec.
 Discharge Temperature above Ambient Temperature 10°C
 ○ - Point of Discharge

SCALE
 in metre : 0 50 100

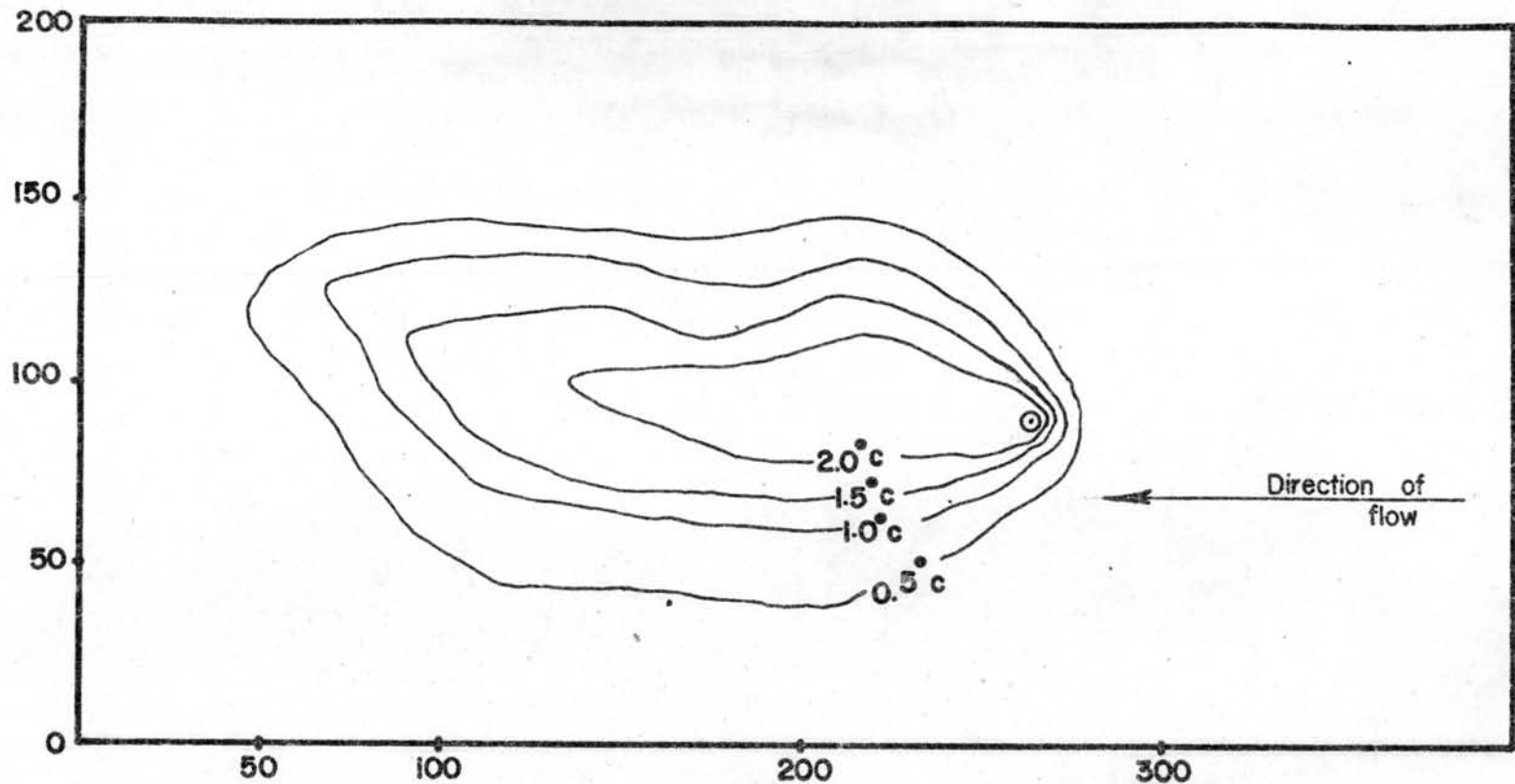
FIG. 5.8 SURFACE TEMPERATURE RISE CONTOURS IN THE VICINITY
 OF THE DISCHARGE FOR RUN NO. 8



Nozzle Diameter 5 meter
 Current Speed 0.9 m/sec
 Discharge Temperature above Ambient Temperature 10°C
 ○ - Point of Discharge

SCALE
 in metre : 0 50 100

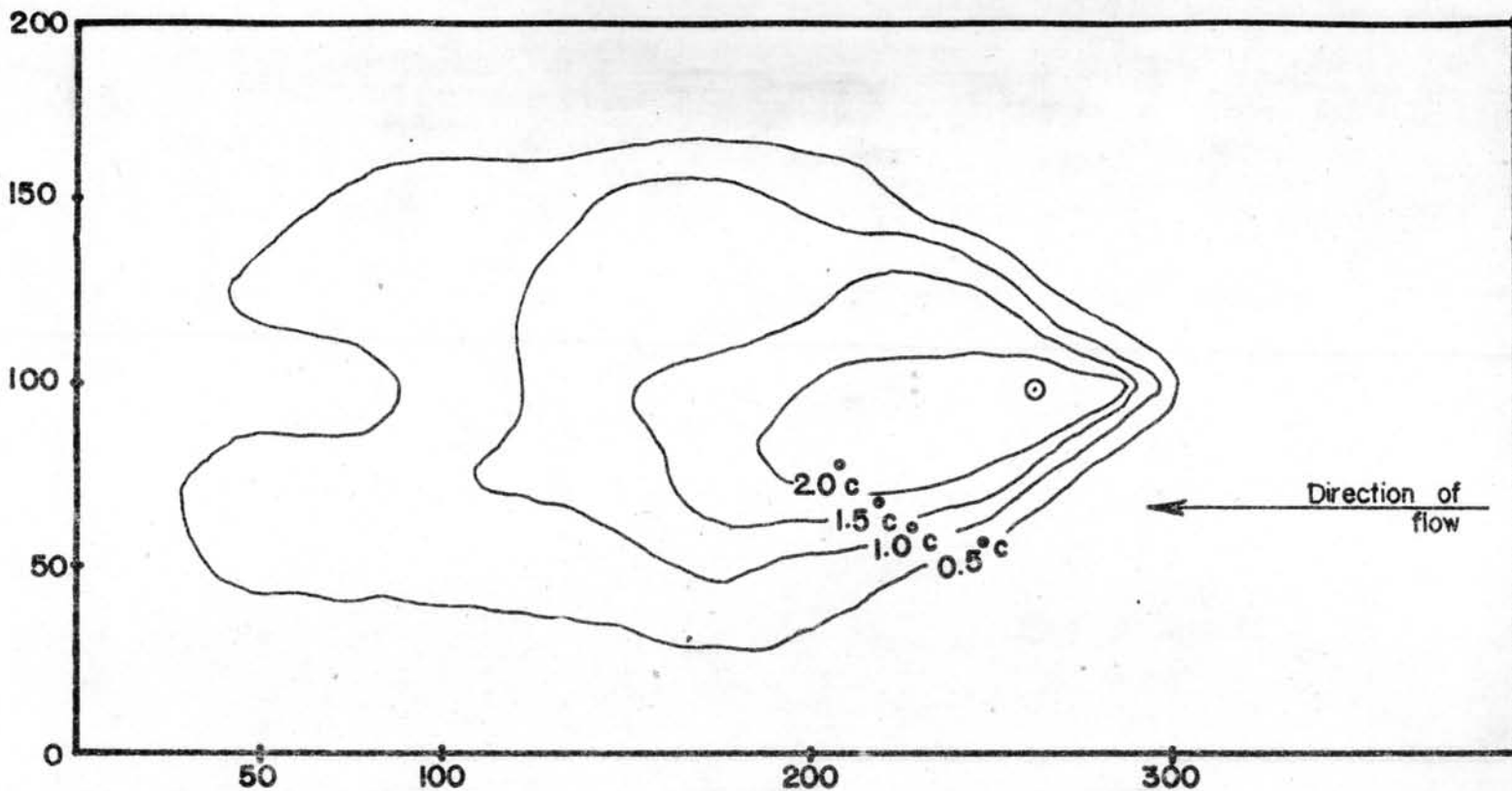
FIG. 5.9 SURFACE TEMPERATURE RISE CONTOURS IN THE VICINITY
 OF THE DISCHARGE FOR RUN NO. 9



Nozzle Diameter 3 metre
 Current Speed 1 m/sec
 Discharge Temperature above Ambient Temperature 10 °c
 ⊙ - Point of Discharge

SCALE.
 in metre 0 50 100

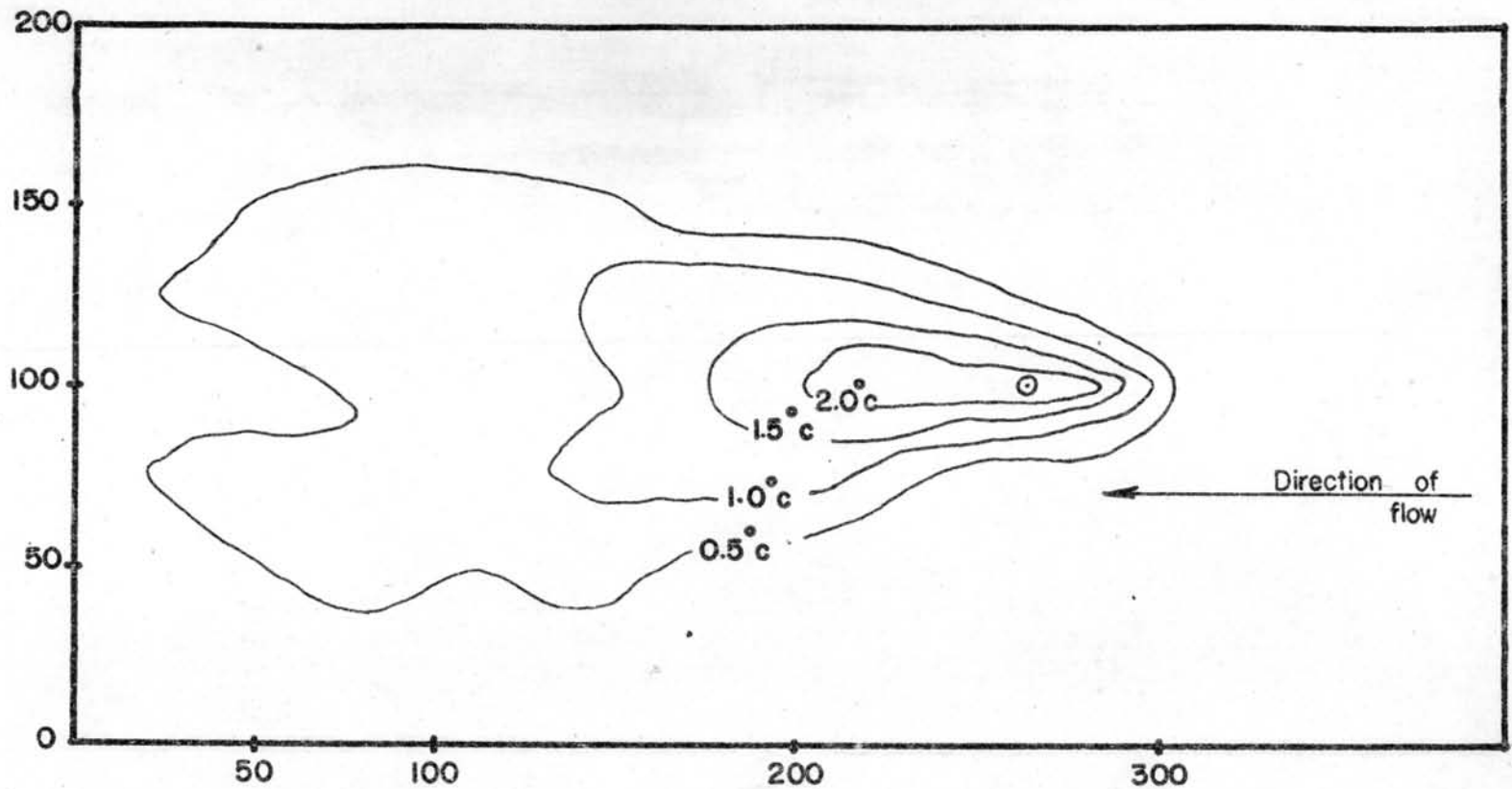
FIG. 5.10 SURFACE TEMPERATURE RISE CONTOURS IN THE VICINITY
 OF THE DISCHARGE FOR RUN NO. 10



Nozzle Diameter 4 metre
Current Speed 1 m/sec
Discharge Temperature above Ambient Temperature 10 °c
○ - Point of Discharge



FIG. 5.11 SURFACE TEMPERATURE RISE CONTOURS IN THE VICINITY OF THE DISCHARGE FOR RUN NO. 11



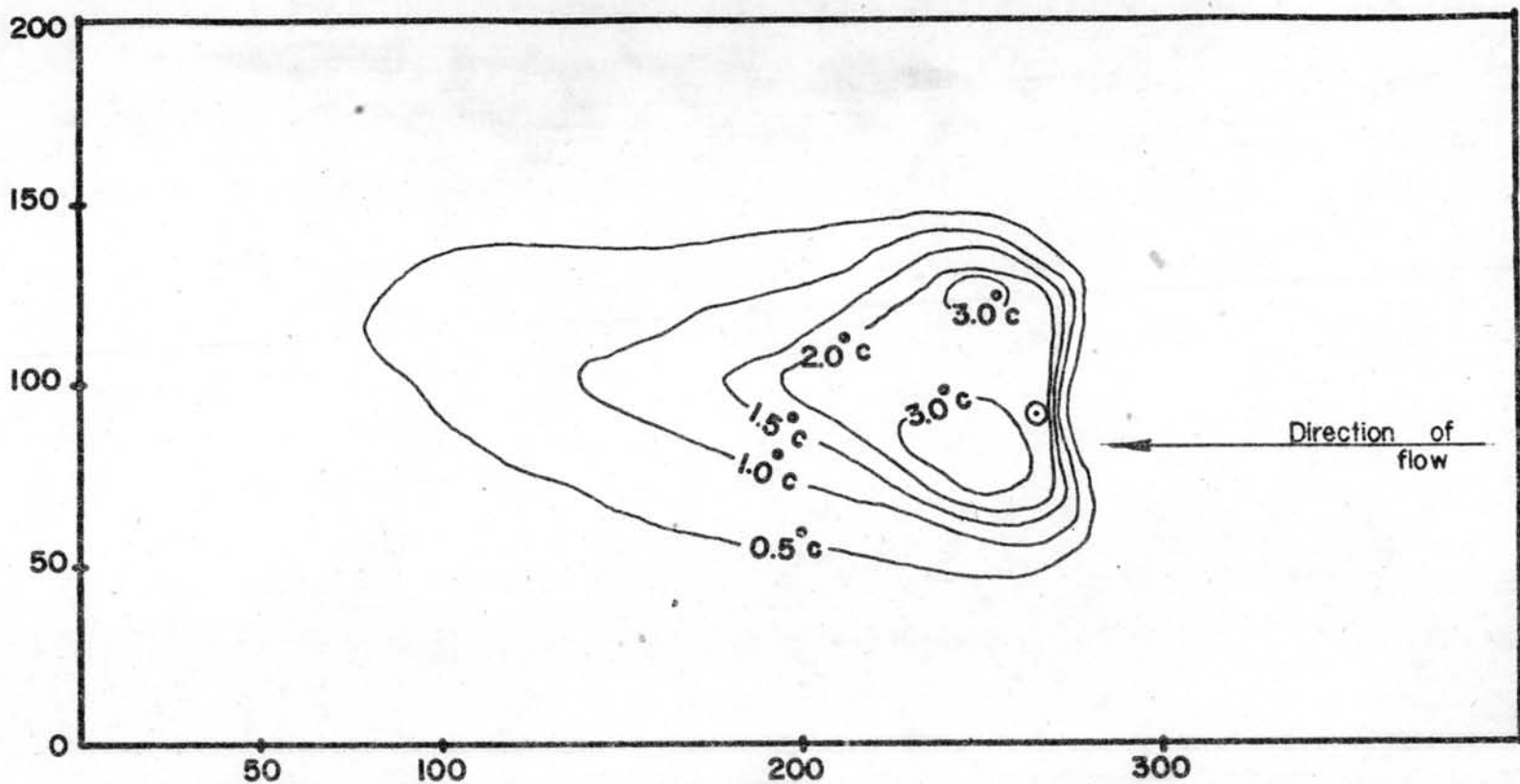
Nozzle Diameter	5	metre
Current Speed	1	m/sec
Discharge Temperature above Ambient	10	° c

⊙ - Point of Discharge

SCALE
in metre



FIG. 5.12 SURFACE TEMPERATURE RISE CONTOURS IN THE VICINITY OF THE DISCHARGE FOR RUN NO. 12

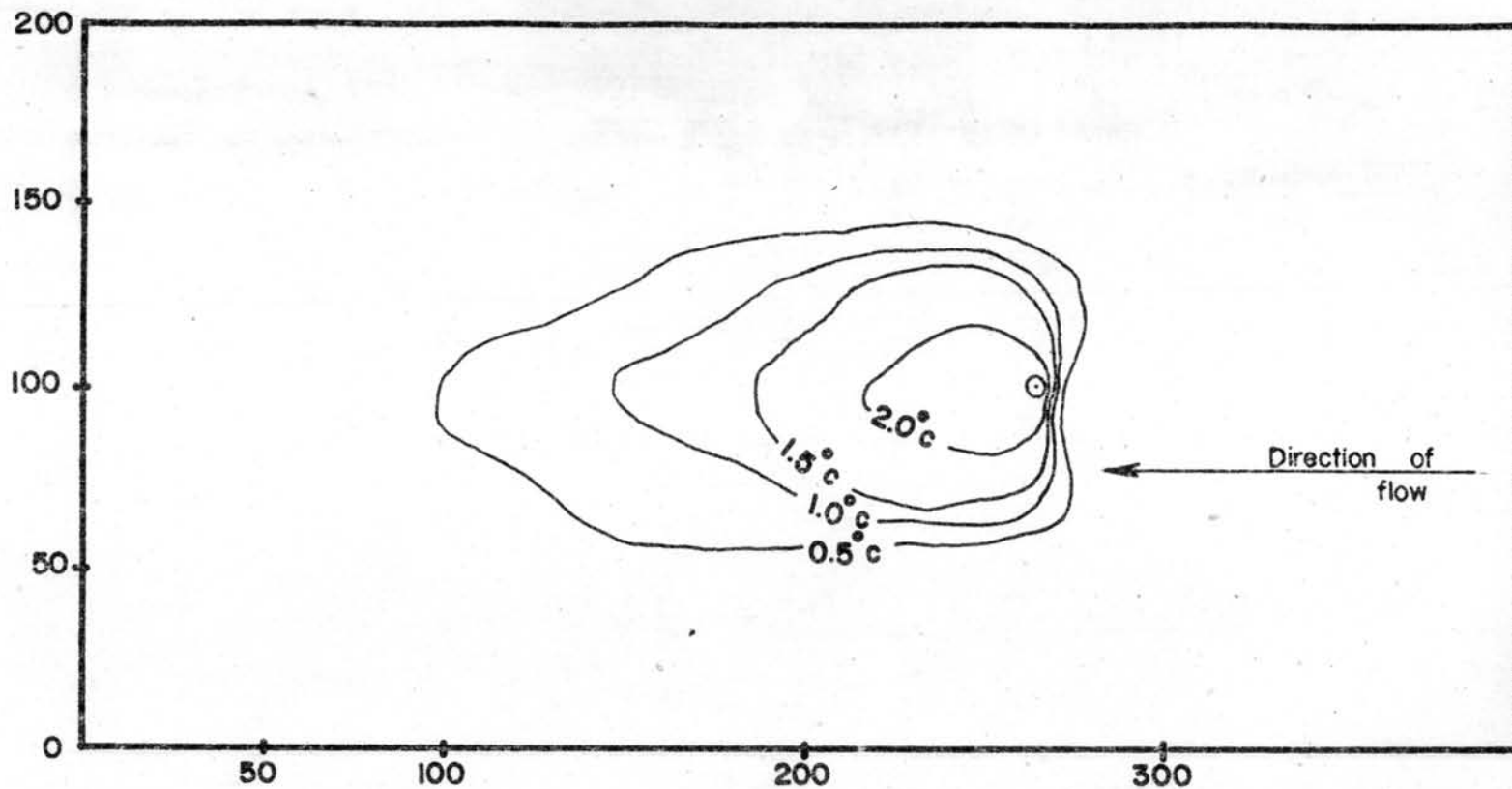


Nozzle Diameter	3	metre
Current Speed	1.2	m/sec
Discharge Temperature above Ambient	10	°c
⊙ - Point of Discharge		

SCALE
in metre :



FIG. 5.13 SURFACE TEMPERATURE RISE CONTOURS IN THE VICINITY OF THE DISCHARGE FOR RUN NO. 13



Nozzle Diameter 4 metre

Current Speed 1.2 m/sec

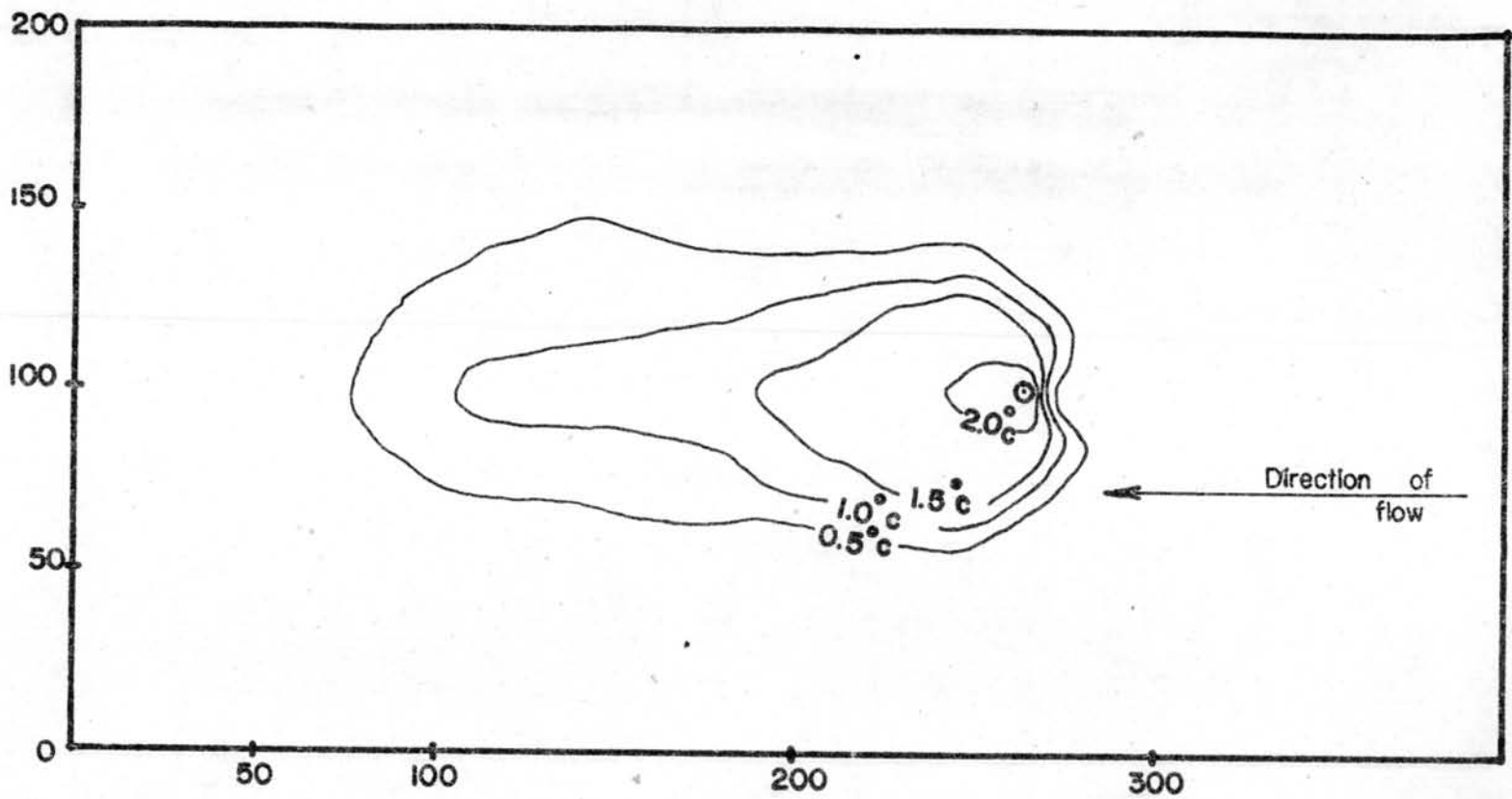
Discharge Temperature above Ambient Temperature 10° c

○ - Point of Discharge

SCALE
in metre :



FIG. 5.14 SURFACE TEMPERATURE RISE CONTOURS IN THE VICINITY OF THE DISCHARGE FOR RUN NO. 14



Nozzle Diameter 5 metre
 Current Speed 1.2 m/sec
 Discharge Temperature above Ambient Temperature 10°C
 ⊙ - Point of Discharge

SCALE
in metre

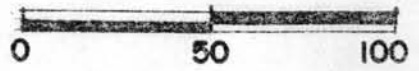
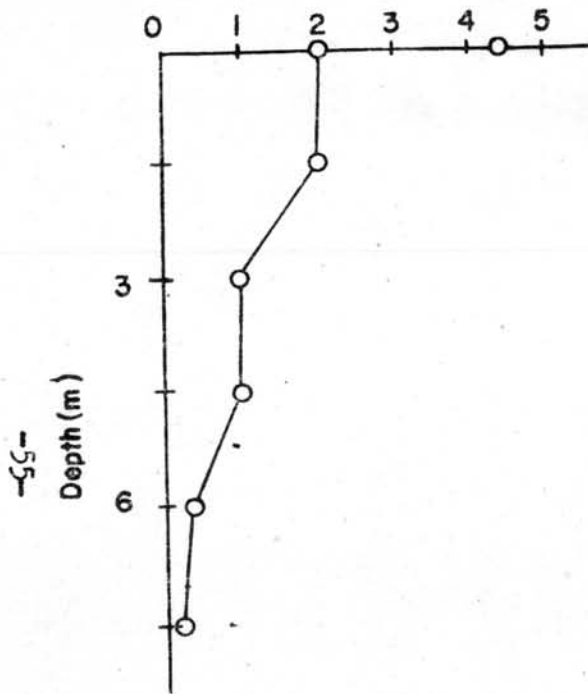


FIG. 5.15 SURFACE TEMPERATURE RISE CONTOURS IN THE VICINITY
 OF THE DISCHARGE FOR RUN NO. 15

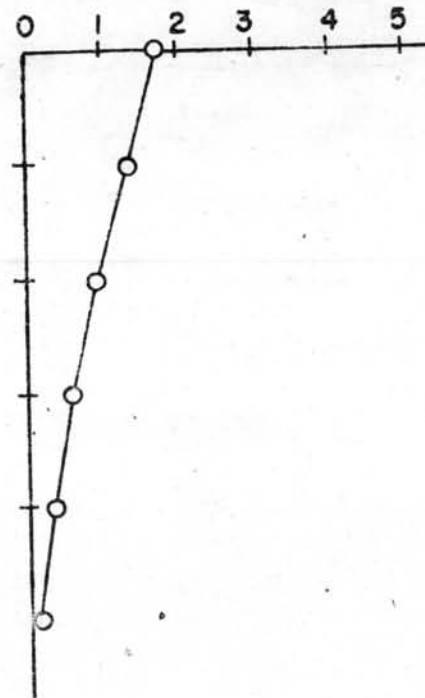
-54-

VERTICAL TEMPERATURE PROFILES

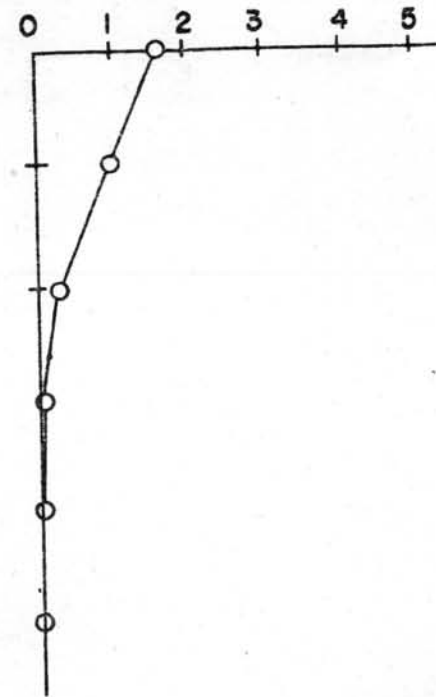
Excess temperature ΔT °C



RUN NO. 1



RUN NO. 2



RUN NO. 3

FIGURE 5.16

Vertical excess temperature profiles at station x (30 m downstream from the point of discharge) for a steady current of 0.6 m/sec

VERTICAL TEMPERATURE PROFILES

EXCESS TEMPERATURE ΔT $^{\circ}\text{C}$

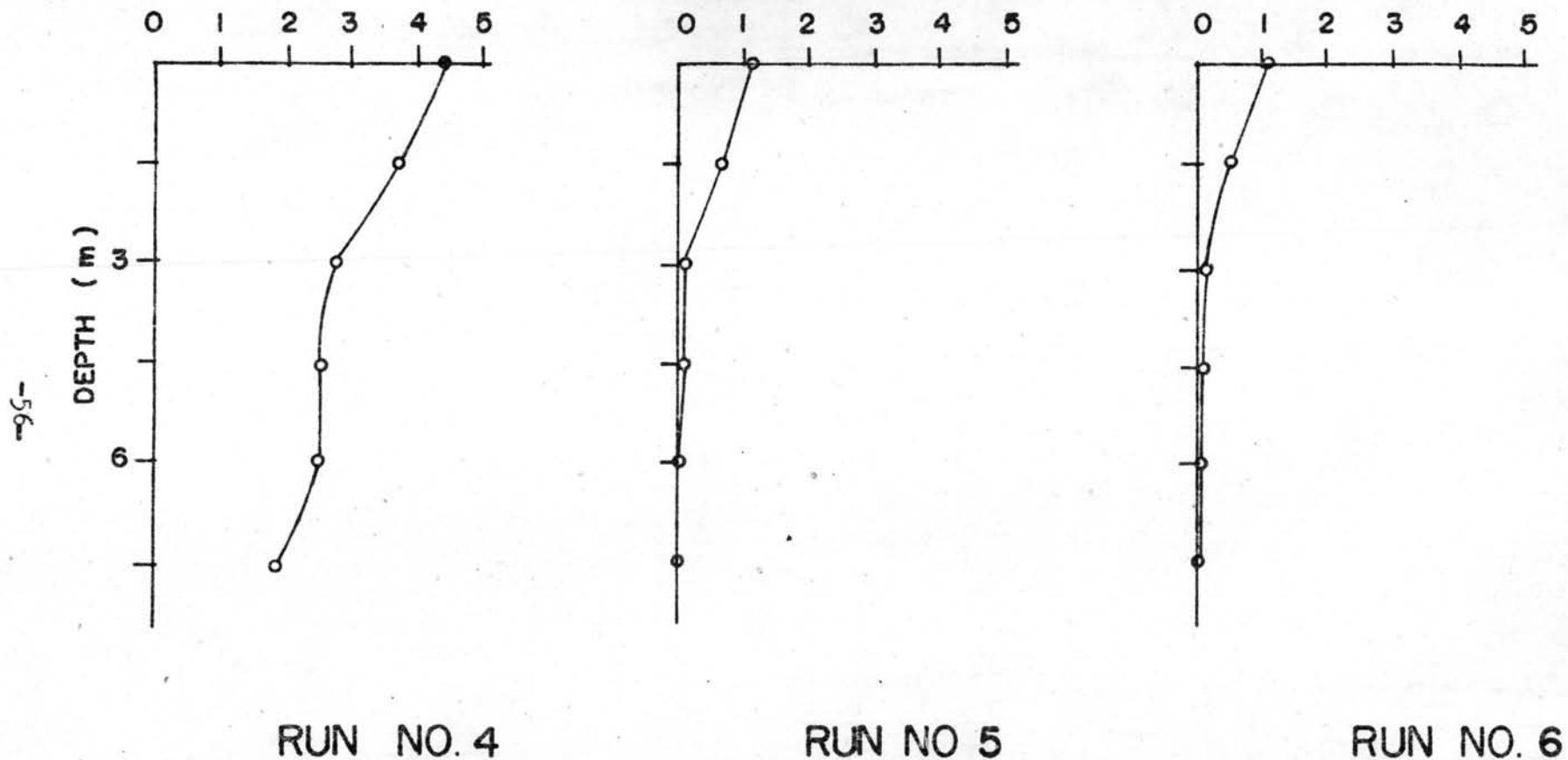
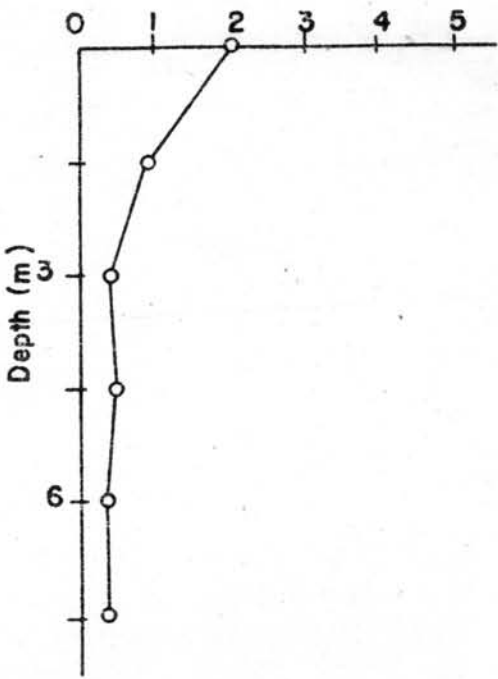


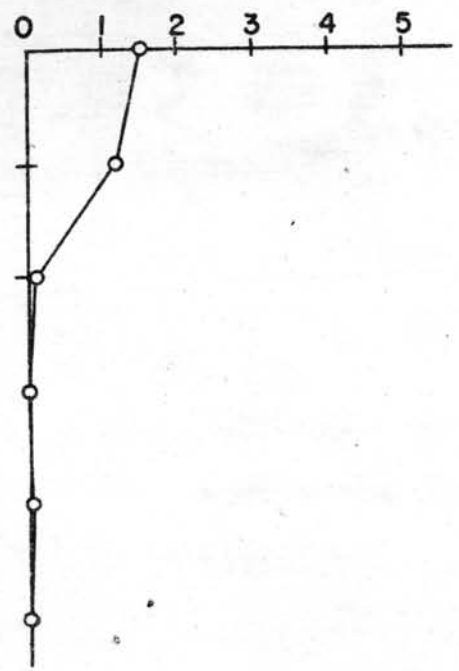
FIGURE 5.17 Vertical excess temperature profiles at station X (30 m. downstream from the point of discharge) For a steady current of 0.8 m / Sec

VERTICAL TEMPERATURE PROFILES

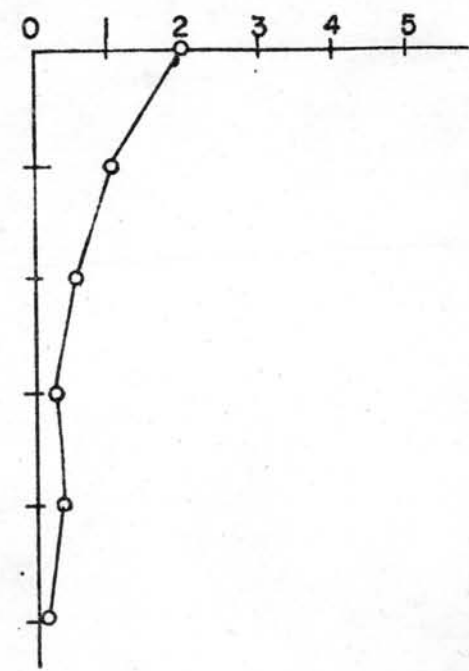
Excess temperature ΔT °C



RUN NO. 7



RUN NO. 8



RUN NO. 9

FIGURE 5.18 Vertical excess temperature profiles at station x (30m downstream from the point of discharge) for a steady current of 0.9 m/sec

VERTICAL TEMPERATURE PROFILES

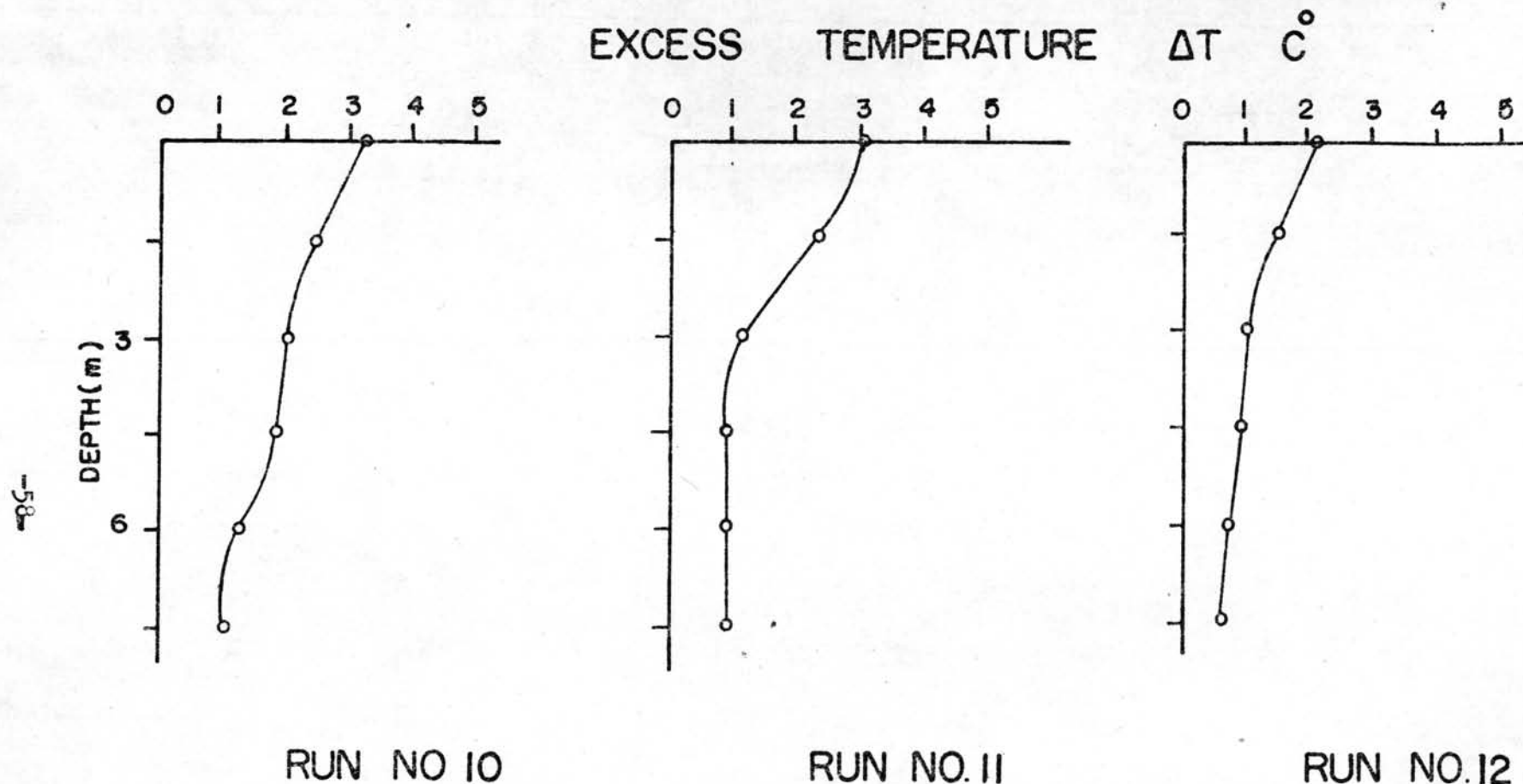
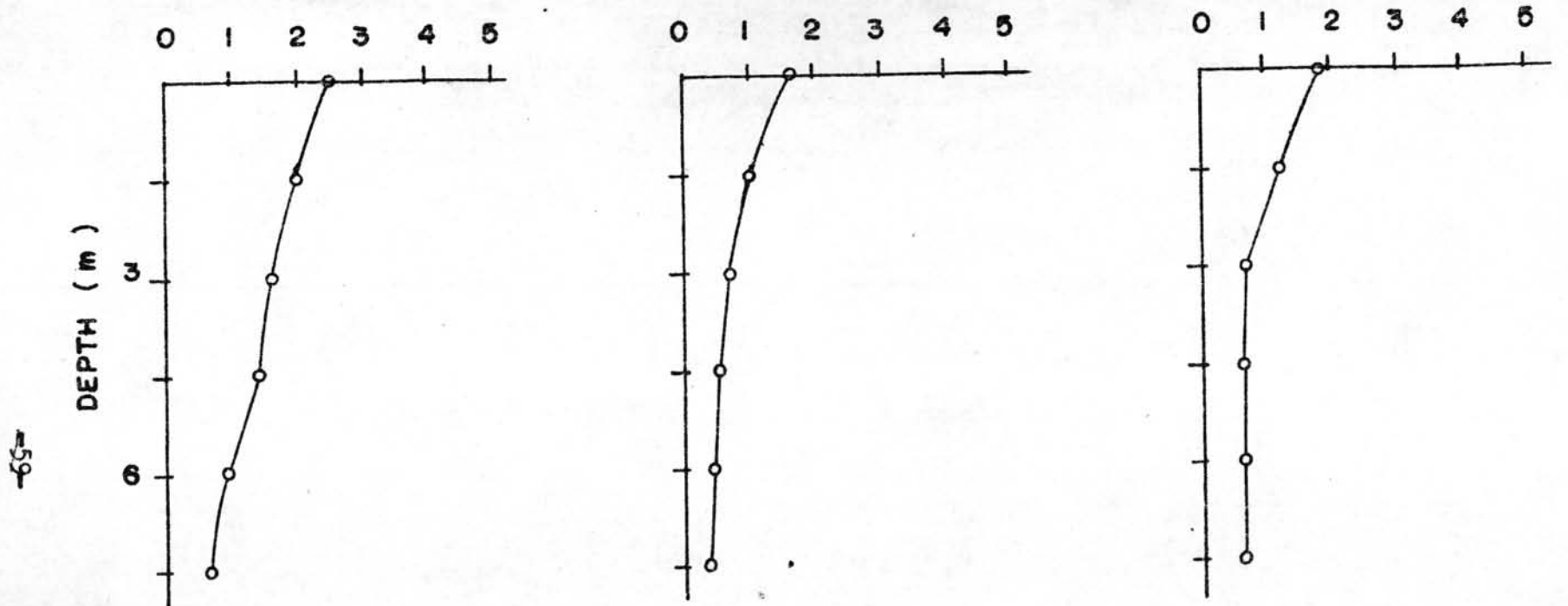


FIGURE 5.19

Vertical excess temperature profiles at station X (30 m. downstream from the point of discharge) For a steady current of 1.0 m/Sec

VERTICAL TEMPERATURE PROFILES

EXCESS TEMPERATURE ΔT $^{\circ}\text{C}$



RUN NO 13

RUN NO 14

RUN NO 15

FIGURE 5.20

Vertical excess temperature profiles at station X (30 m. downstream from the point of discharge) For a steady current of 1.2 m / Sec

5.2 Effect of current speed.

Five values of current speed, 0.6, 0.8, 0.9, 1.0 and 1.2 m/sec, were employed in the investigation. For 3 m. nozzle diameter, the study shows that, when the areas of the same isothermal lines are plotted against the values of current speed (Fig. 5.21), the mixing zone varies inversely with current and has the relation which is in the form of the straight line. That is, as the current increases, the area of the mixing zone decreases. This is because when the current is faster, the volume of ambient water entrained is also greater. Consequently dilution of the hot water will be more effective.

The slope of the straight lines for various isothermal areas are not the same as shown in Fig. 5.21 . They tend to meet together at the high current speed. This means that the isothermal lines representing each temperature are very close to each other.

Further experimental runs using 4.0 and 5.0 m. nozzle diameter leads to the same conclusion. Figures 5.22 - 5.23 illustrate the relation between the measured mixing zone and the current speed for 4.0 and 5.0 m. nozzle diameter respectively.

5.3 Effect of the size of nozzle.

The effect of the size of nozzle on the temperature distribution may be illustrated by plotting, for each nozzle, the mixing zone encircled by 2°C isothermal line against the current speed. The results displayed in Fig. 5.24 indicates that, as the size of the nozzle decreases, the area of the mixing zone increases. This is true for most values of U except in the region where U is less than 0.9 m/sec .

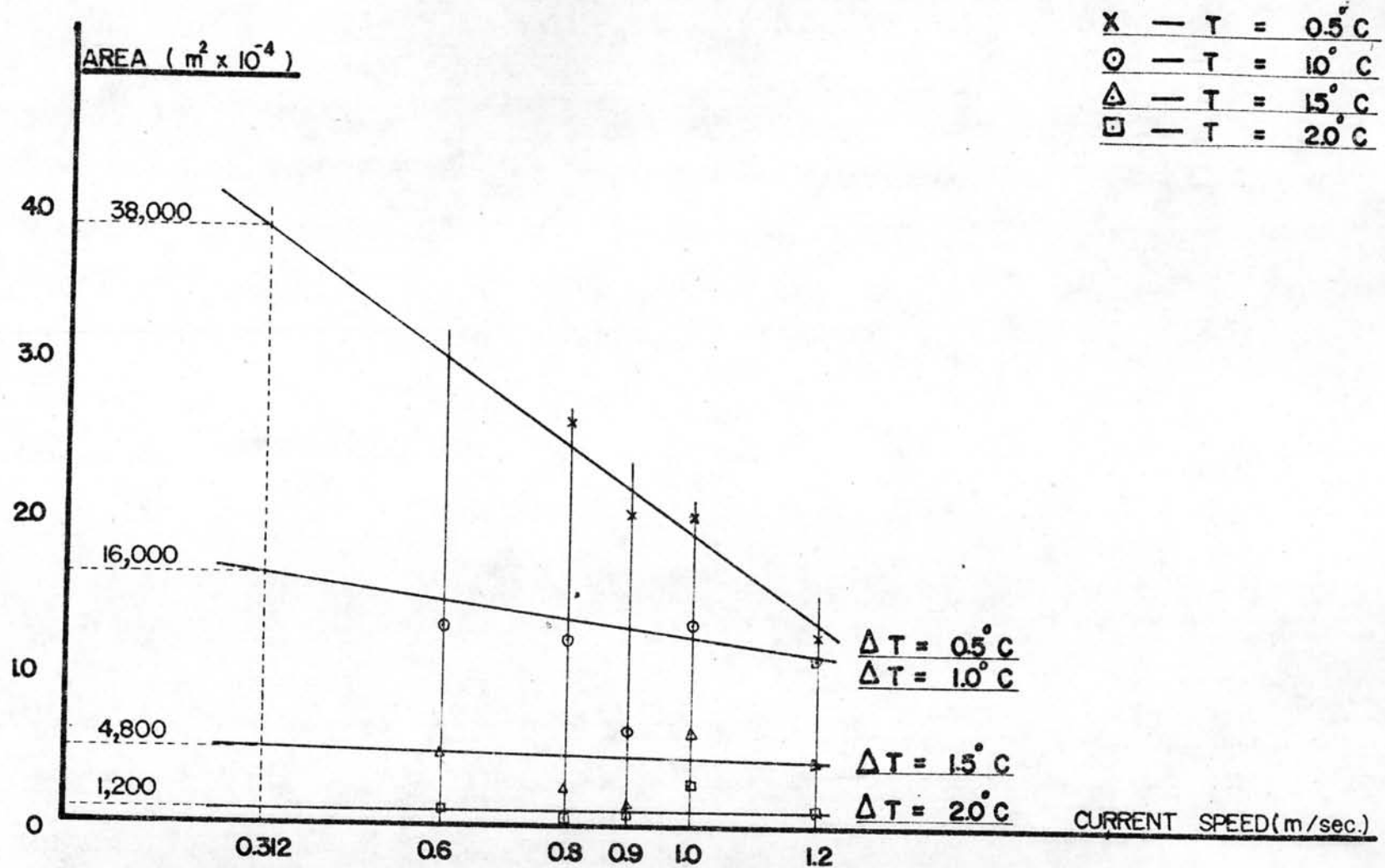


FIGURE 5.22

RELATION BETWEEN THE AREA OF THE ISOTHERM AND CURRENT SPEED (4 METRES NOZZLE DIAMETER.)

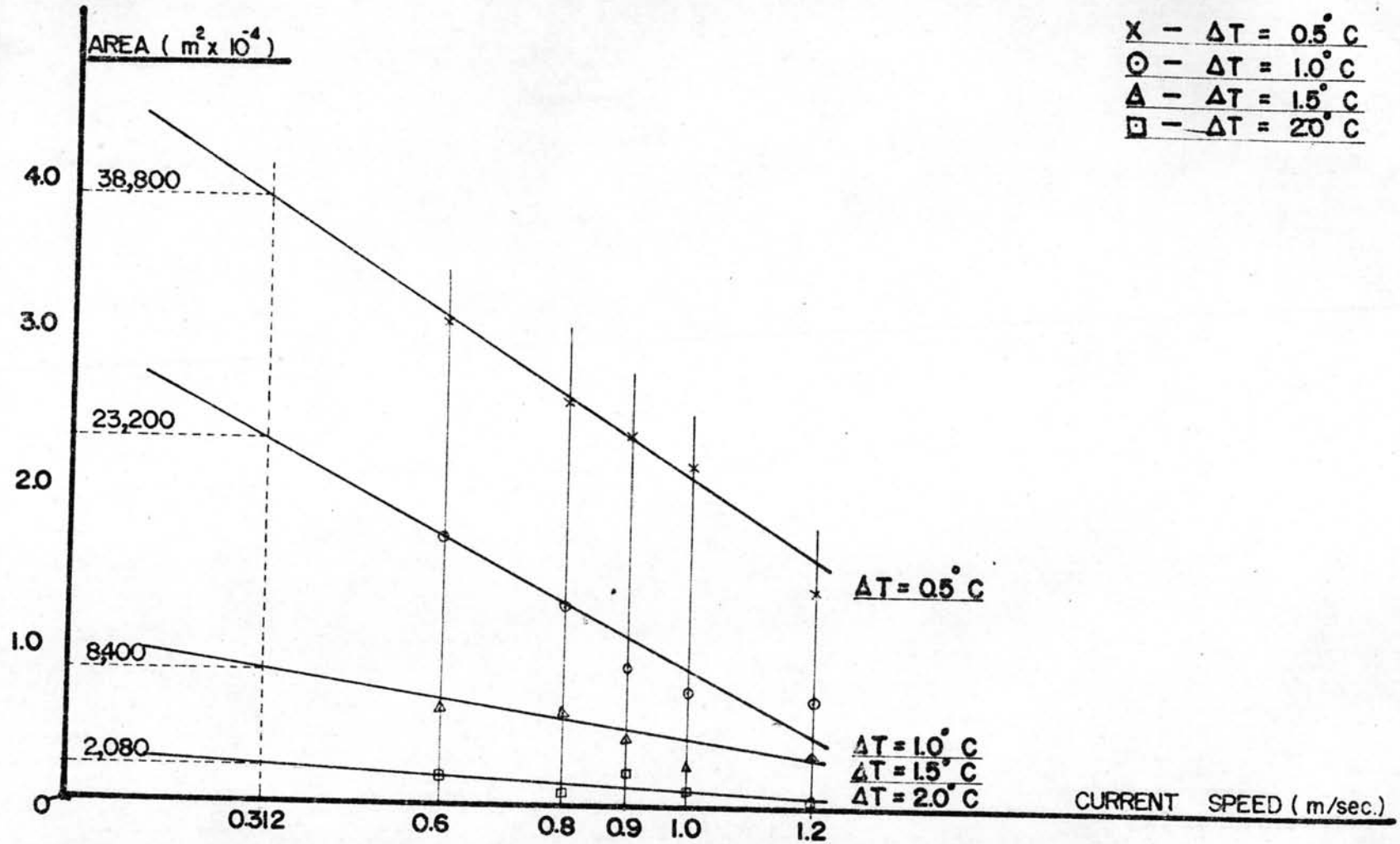


FIGURE 5.23

RELATION BETWEEN THE AREA OF THE ISOTHERM AND CURRENT SPEED (5 METRES NOZZLE DIAMETER.)

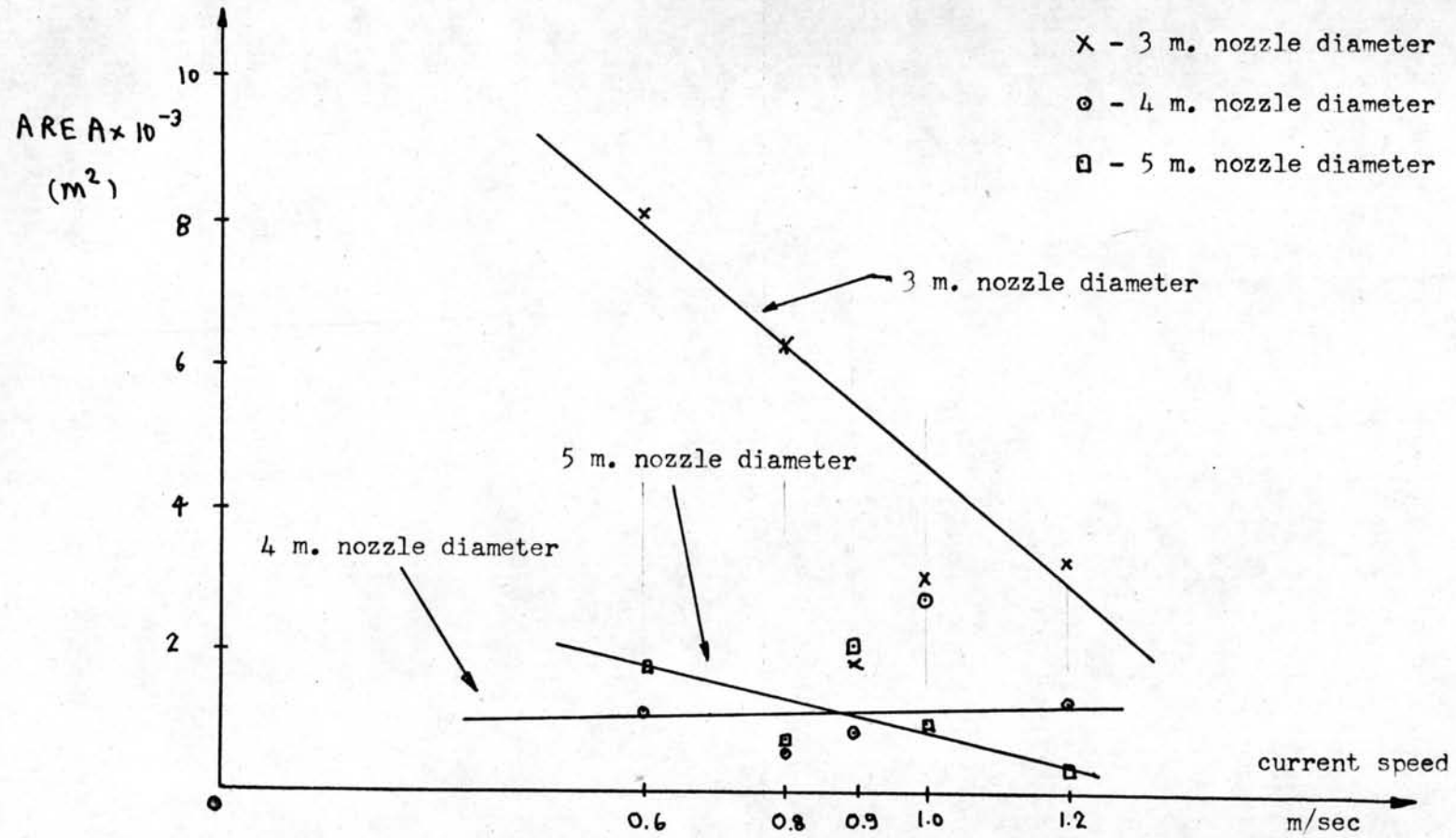


Fig. 5.24 Relation between the area of 2 C isotherm and the current speed.

In this case the mixing zone obtained using 4 m. nozzle diameter is smaller than that using the 5 m. nozzle diameter. This means that the effect of increasing the nozzle diameter will generally increase the rate of entrainment, but as the nozzle diameter is further increased, the decrease in the length of the jet trajectory (jet velocity varies inversely with the nozzle diameter) will counter-balance the increase in the entrainment rate and eventually lower the jet dilution.

5.4 Vertical temperature.

At the point 30 m. downstream from the discharge point, the temperature of six different locations at various depths (1.5 m. apart) were measured. From the results shown in Figures 5.16 through 5.20 , it may be observed that the temperature is highest at the water surface. Also, the temperature decreases as the depth increases. This means that the jet momentum of the discharge has insignificant effect on the temperature field. Otherwise, the temperature should increase with the depth increases.

5.5 Comparison between the experimental and predicted values of the surface temperature.

Figure 5.25 illustrates the comparison of the surface temperature between the experimental and predicted values for a given current speed of 1.0 m/sec (see Table 3.1). The discrepancies observed may be attributable to the following two factors. Firstly the prediction equation assumes linear and non-dispersive nature of phenomenon which contradicts the reality. Secondly the heat dissipation parameter, λ , was set equal to $58.6 \text{ cal/cm}^2 \cdot \text{hr} \cdot ^\circ\text{C}$, a value recommended for the case in which the

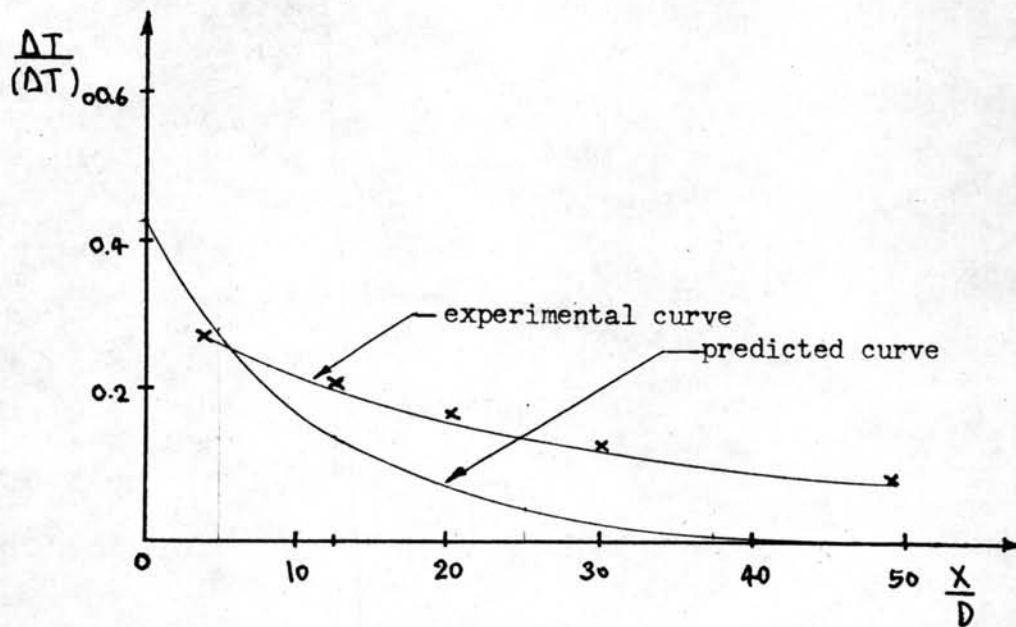


Fig. 5.25 Comparison of the surface temperature between the experimental and predicted values.

test is performed outdoor. In the present experiment, λ should take a smaller value and consequently, the predicted distribution of ΔT should move closer to the experimental curve.

5.6 Estimated temperature distribution for the case of low current speed.

In the present work, experiments were carried out using the currents between 0.6 to 1.2 m/sec . But at the location of the proposed Nuclear Power Plant, the average current speed recorded by EGAT is 0.312 m/sec . To obtain the mixing zones at this low current of 0.312 m/sec , extrapolation of the relation between the mixing zone and current speed (Fig. 5.21 - 5.23) is required. Table 5.3

illustrates the corresponding areas within various isothermal lines at the required average current velocity.

TABLE 5.3

ESTIMATED AREAS WITHIN VARIOUS ISOTHERMAL
LINES AT THE AVERAGE CURRENT VELOCITY

Current velocity (m/sec)	Nozzle Diameter (m)	Areas within isothermal lines (m ²)			
		$\Delta T = 0.5$	$\Delta T = 1.0$	$\Delta T = 1.5$	$\Delta T = 2.0$
0.312	3	36,400	26,000	20,000	10,800
0.312	4	38,000	16,000	4,800	1,200
0.312	5	38,800	23,200	8,400	2,080